Indian Journal of Fibre & Textile Research
Vol 47, March 2022, pp. 190-198

Electromagnetic interference shielding performance of 3-D spacer fabric coated with reduced graphene oxide/carbon nanotubes

Zhang Man-ning[a], Zhong Zhi-li, Rong Xiang & Cai Jie

School of Textile Science and Engineering, Tianjin Polytechnic University, Tianjin 300387, China

Received 11 November 2020; revised received and accepted 12 August 2021

In this work, a new type of three-dimensional spacer woven fabric (3DSWF) has been designed, whose upper and lower layers are of interlaminar orthogonal structure. These two layers are connected well with spacing yarns interweaved with weft yarns and arranged in an 'X' shape in the spacing layer. In order to expand the application field of 3DSWF, reduced graphene oxide (rGO) and carbon nanotubes (CNTs) coated 3DSWFs are prepared. The synergistic effect between rGO and CNTs gives 3DSWFs excellent electrical conductivity and electromagnetic interference (EMI) shielding performance. The results show that the layer-by-layer assemble method is conducive to play the synergistic effect between rGO and CNTs. The EMI shielding effectiveness of sample can reach to 15 dB from 2 dB in the frequency range of 0-3GHz. Besides the electrical conductivity, the preparation method is also one of the factors affecting the EMI shielding performance of coated 3DSWFs. This study provides idea for the design and preparation of 3DSWF and further developing 3DSWF-based materials with multiple functions.

Keywords: Carbon nanotubes, Electrical conductivity, EMI shielding performance, Nylon yarn, Reduced graphene oxide, Space fabric, Three-dimensional fabric

1 Introduction

With the begining of the era of 5th-Generation, there is a worldwide concern that the large amount of electromagnetic waves generated by electronic devices affects the normal operation of other equipments and even threaten the health and safety of life[1-3]. The demand for electromagnetic interference (EMI) shielding fabrics has increased dramatically in all industries, due to their flexible, light weight, permeability and tailorability, characteristics that can be uesd on the complex shapes and for promising potential applications in portable electronics and wearable smart textiles[4-6]. To date, many efforts have been made to develop fabrics with high EMI shielding performance by introducing matels , carbon based materials and conductive polymers[7-13].

Carbon nanotubes (CNTs), as a one-dimensional carbon nanomaterial, have high aspect ratios allowing them to combine with fabrics to form a complete uniform conductive network with less load[14,15]. However, due to the poor dispersion of CNTs in the matrix, it is difficult for pure CNTs to construct an effective conductive network. Chen *et al.*[16] added Py-β-CD to CNT to combine the two via π-π bond to form a stable suspension and then coated it on nonwoven fabric. Xu *et al.*[17] deposited the Cu nanolayer on the CNT film, and obtained the flexible material with shielding effectiveness (SE) greater than 50 dB.

Graphene's special multilayered structure gives the ability to absorb electromagnetic waves, but its hydrophobicity makes it difficult to combine with other materials[18]. The oxygen-containing groups of graphene oxide (GO) are favorable for its grafting on the fabric through the formation of hydrogen bonds and Van der Waals forces, but reduced-treated rGO is much less conductive than graphene due to changes in its crystal structure and the remaining oxygen-containing groups[19]. To overcome this problem, many researchers have introduced other materials into rGO[20,21]. In terms of structure, as compared with zero-dimensional spherical metal nanoparticals, the combination of one-dimensional material and two-dimensional material is more conducive to the formation of complete three-dimensional conductive network[22-24]. In order to improve the electrical conductivity and EMI shielding properties of fabric, CNTs and rGO are used together as conductive materials.

The three-dimensional spacer woven fabric (3DSWF) has two independent upper and lower

[a]Corresponding author.
E-mail: 1344586260@qq.com

layers, which are connected by spacing yarn with a certain height, thus forming a integrated hollow sandwich structure[25-30]. At present, the 3DSWF is most widely studied because of its outstanding mechnical properties[26,31,32]. To the best of our knowledge, there are few studies available on direct use of 3DSWF as EMI shielding matrix, which is more widely used to obtain excellent mechanical properties and sound absorption properties[33,34]. Therefore, it's necessary to develop a multifunctional 3DSWF including EMI shielding performance, which will have a wide range of application prospects and development potential.

In this study, a new 3DSWF with special structure has been designed, using CNTs and rGO as conductive materials. CNTs and rGO are combined with 3DSWF by two methods to offer insulated 3DSWF conductivity and EMI shielding properties. Meanwhile, the effects of two different preparation methods on the electrical conductivity and EMI shielding property of the 3DSWF are studied. The results show that there is synergistic interaction between CNTs and rGO, and the layer-by-layer assemble method is more conducive to the synergy of them. After being coated, the spacing yarn of 3DSWF can work as a 'bridge' to connect the two surfaces to make the coated 3DSWFs as a whole conductive. The purpose of this work is to broden the application scope of 3DSWF.

2 Materials and Methods

2.1 Materials

Nylon yarn of Gold Three Fishes Brand (210D/3 strands of yarn) was obtained. Multiwalled carbon nanotubes (CNTs) dispersion at 10% concentration (10-30 μm length and 5-10 nm diameter) as well as graphene oxide (GO) dispersion at 5 mg/mL concentration were perchased from Tanfeng Tech.Inc. L-ascorbic acid (L-AA) was obtained from Fuchen (Tianjin) Chemical Reagent Co. Ltd. Ethanol absolute was obtained from Damao Chemical Reagent Factory.

2.2 Design and Configeration of 3DSWF

In this study, nylon yarns were used as warp, weft and spacing yarns to fabricate the three-dimensional spacer woven fabric (3DSWF) on a Semi-automatic sample loom. The organization diagram of 3DSWF is shown in Fig. 1(a). There are 10 columns, in which 1-4 and 5-8 represent the ground warp of upper layer and lower layer respectively, 9 and 10 represent the spacing yarn, the warp points formed by the interlacing of ground warp and weft are marked as ■, and the warp points formed by the interlacing of jointed warp and weft are marked as Δ.

For this 3DSWF, the density of spacing yarns can be changed according to the need in the design of the weave structure, and the thickness of sample can be adjusted by changing the height of spacing yarns in the weaving process. In this work, the 3DSWF is

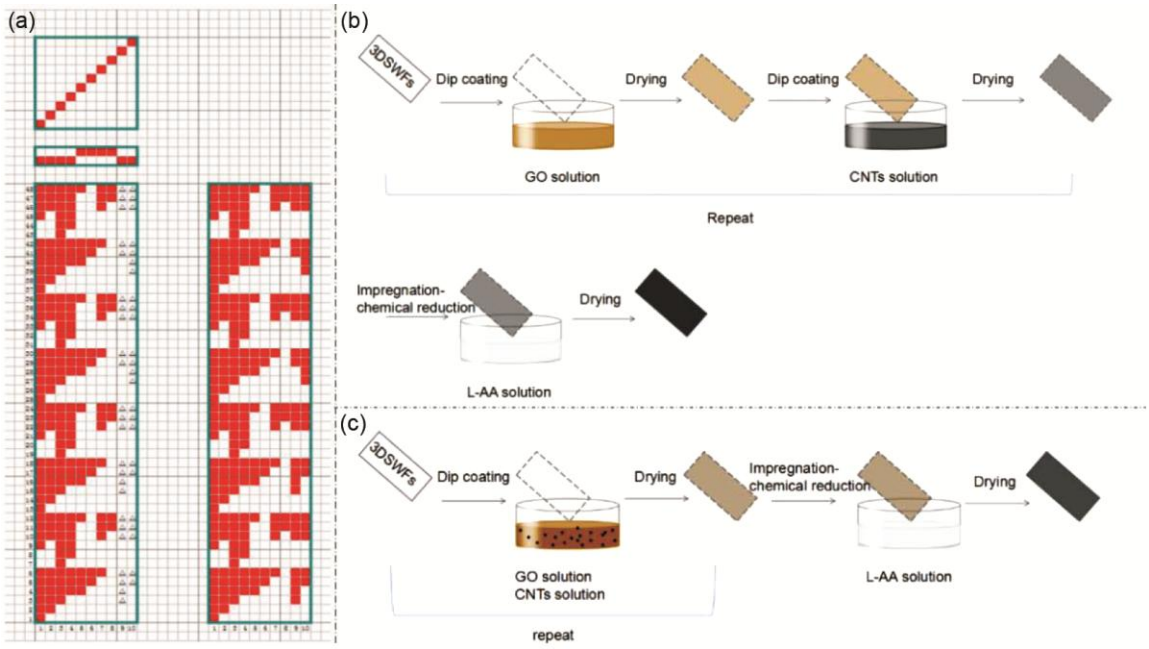

Fig. 1 — (a) Organization diagram of 3DSWF; and schematic illustration of preparation of coated 3DSWFs (b) CNTs/rGO/3DSWFs and (c) CNTs@rGO/3DSWFs

designed, keeping spacing yarn density 30 roots/cm^2 and spacing yarn height 3mm.

2.3 CNTs/rGO Coated 3DSWFs Preparation

Layer-by-Layer Assembly Method

Before the fabrication, all samples were first cleaned by a sonicator in 200 mg/L ethanol solution for 30 min to remove the residual impurities in 3DSWF and then dried. The schematic diagram of the CNTs/rGO coated 3DSWFs preparation by layer-by-layer assembly method is shown in Fig. 1 (b).

The GO suspension was diluted by adding distilled water (dipping Solution A), and the CNTs suspensions of various concentrations were prepared by adding some volume of distilled water (dipping Solution B). The mass of L-AA was weighed, diluted with distilled water (the mass ratio of L-AA to GO 15:1), and then used as the reduction treatment (Solution C), the bath ratio of all solutions was kept 1:50.

Firstly, the CNTs/GO coated 3DSWFs were prepared by layer-by-layer assembly method. Typically, the pretreated samples were first soaked in Solution A to absorb GO and then dried at 120℃. After that the 3DSWF was put into Solution B and then dried at 120° C. In this context, one layer of GO and CNTs was obtained in one deposition cycle. By repeating these immersed and drying steps six times, multilayered CNTs/GO coating was constructed.

Finally, the CNTs/rGO coated 3DSWFs were prepared by chemical reduction. The dried CNTs/GO coated 3DSWFs were immersed in Solution C for 2h at 100℃ in a water bath and then dried at 120℃ in an oven to obtain the CNTs/rGO coated 3DSWFs.

In-one-bath Method

The schematic diagram of the CNTs@rGO coated 3DSWF, prepared using in-one-bath method, is shown in Fig. 1 (c).

A required amount of GO suspension and CNTs dispersion was measured respectively and then poured into flask, then distilled water was added to dilute it to the target concentration, keeping the bath ratio 1:50. Then it was treated with ultrasonic for 1h to make it evenly dispersed as the dipping solution. Among them, the preparation method of GO solution and CNTs solution were the same as those in Layer-by-Layer assembly method.

Firstly, the CNTs@GO coated 3DSWFs were prepared by in-one-bath method. Typically, the pretreated samples were soaked in dipping solution to absorb GO and CNTs then dried at 120℃, by repeating these immersed and drying steps nine times, multilayered CNTs@GO coating was constructed.

Finally, the CNTs@rGO coated 3DSWFs were prepared using the same treatment as shown in Layer-by-Layer assembly method for chemical reduction.

Samples of 3DSWFs coated separately with rGO or CNTs were also prepared for comparison. The surface resistance (SR) of samples was selected as dependent variable, and the preparation process parameters were determined by single factor analysis method, including concentration of GO solution, immersion time and number of coating, reductant content, reduction time & temperature, and layer-by-layer assembly concentration of CNTs solution, immersion time and number of coating.

2.4 Characterization

Microstructure of 3DSWF and coated 3DSWFs with conducting layer was detected with field-emission scanning electron microscope (FE-SEM TM3030) at an accelerating voltage of 30 kV, each specimen was coated with gold prior to the observation.

The double electrical four-probe meter (PTS-9 type) was used to measure the electrical resistivity of coated 3DSWFs at the current range of 10 μA. After placing the sample on the panel and adjusting the knob to contact the probe with the sample surface, every sample was tested 10 times at different positions to reduce error and then the average value was recorded.

The Rohde & Schwarz ZNB40 type vector network analyzer was used to measure EMI shielding effectiveness of coated 3DSWFs with conductive materials in the frequency range of 0-3 GHz.

3 Results and Discussion

3.1 Weaving and Forming

The fabric structure diagram and the actual photo of 3DSWF are shown in Fig. 2. Figure 2 (a) shows the fabric structure of upper and lower layer, while Figs 2(b) and (c) show the elevation and left view of 3DSWF, Figure 2 (d) is the photo of 3DSWF. It can be noted that the face sheets of 3DSWF are woven by warp and weft yarns as interlaminar orthogonal structure, and the spacer layers of 3DSWF are consisted of spacing yarns arranged in an ‘X’ shape. The spacing yarns are interweaved with the weft of the upper and lower layers along the warp direction

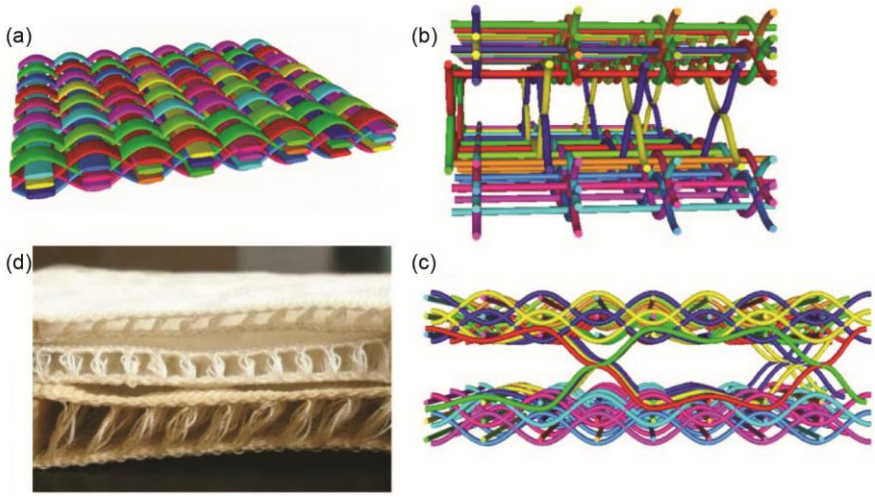

Fig. 2 — Fabric structure diagram (a) upper and lower layer construction, (b) left view of 3DSWF structure, (c) elevation view of 3DSWF structure, and (d) actual photo of 3DSWF

according to certain rules, making the 3DSWF as a whole.

3.2 Determination of Prparation Process Parameters

Surface resistance (SR) of the sample was taken as the dependent variable and the single factor analysis method was used to select the best preparation parameters. The test results are shown in Fig. 3.

Figures 3 (a)-(c) show the influence of preparation process parameters on SR of the 3DSWFs coated with GO solution only. As shown in Fig. 3 (a), with the increase in concentration of GO solution, the SR of sample drops quickly. When the concentration reaches to 3 mg/mL, the SR decreases to 0.47MΩ, and finally as the concentration continues to increase, the SR flattens out. Figure 3 (b) shows the influence of the immersion time of the sample in GO solution on the SR. The SR decreases with the increase in immersion time, and the SR reaches to minimum value (0.06MΩ) after 2h of immersion, After that when time continues to extend, the SR increases. This phenomenon indicates that when soaked for 2h, the laminate GO can no longer enter the 3DSWFs interior but accumulates on its surface, which has a bad effect on the electrical conductivity of the samples. Figure 3 (c) shows that SR drops rapidly when coated 3 times. When coating is increased to 9 times the SR reduction rate becomes slow and the value reaches to 0.43KΩ. On further increase in the number of coating the SR remains almost unchanged. Therefore, the optimum concentration, immersion time and number of coating of GO solution are 3 mg/mL, 2 h and 9 layers respectively.

Based on the determination of rGO process, the influence of the concentration of CNTs solution, immersion time and number of coating on SR of samples has also been analyzed using layer-by-layer assembly method, and the results are shown in Figs. 3 (d)-(f). As shown in Fig. 3 (d), the SR of sample decreases with the increase in CNTs solution concentration. At the concentration of 2 mg/mL, the SR decreases to 9.65KΩ. When concentration is further increased, SR drops slowly. This is because, with the increase of CNTs concentration, the conductive network on the samples becomes more complete, the number of free electron increases, and the conduction current also strengthen. Hence, the resistivity of the sample decreases. Considering that the preparation process parameters used in two methods should be consistent, and the increase of CNTs solution concentration in one-bath method will further increase the viscosity of the dipping solution; hence 2 mg/mL is used as the optimum concentration of CNTs solution. Figure 3 (e) shows that the SR decreases with the increase in immersion time and the SR is reached to minimum value (9.85KΩ) after 30 min of immersion, when immersion time continues to extend, the SR increases. This suggests that the individual CNTs will creat agglomerations in some parts of the GO surface and remaining 3DSWFs surface after 30 min of coating. Figure 3 (f) shows that the SR decreases with the increase in coating layer. For 6 layers coated sample, SR falls to 0.57KΩ. To sum up, the optimum concentration, immersion time and coating number of CNTs solution are set as 2 mg/mL, 30 min and 6 layers respectively.

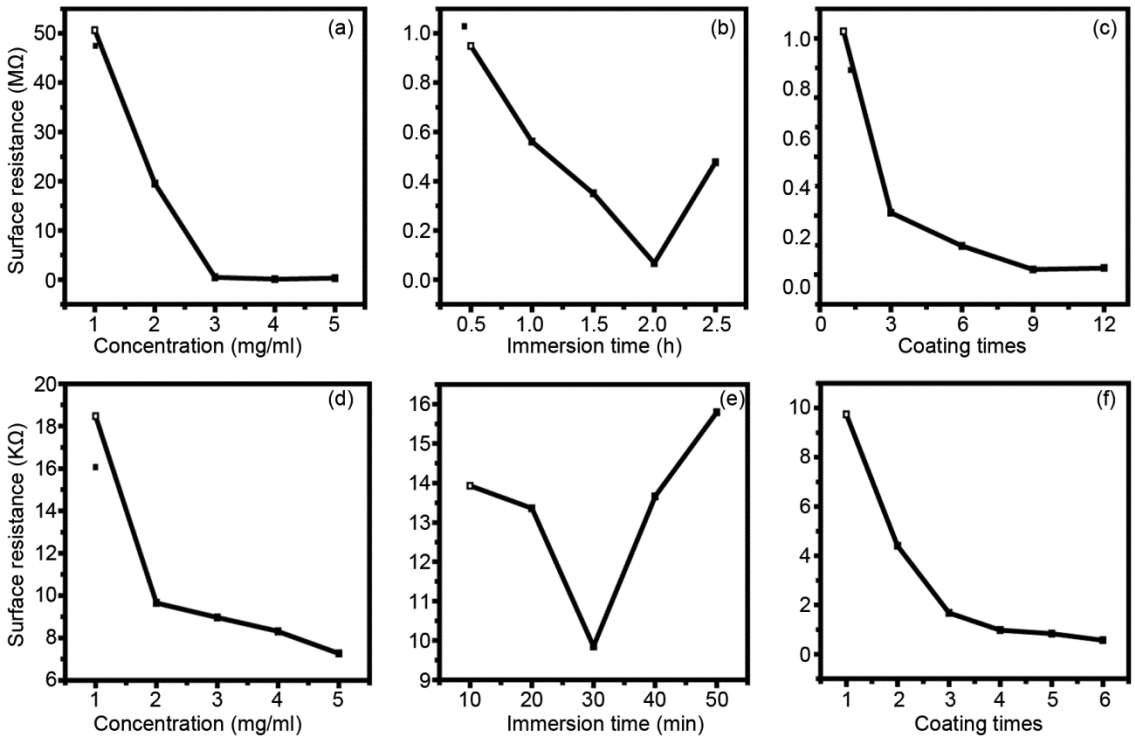

Fig. 3 — Test results obtained by single factor analysis method for layer-by-layer assembly (a&d) concentration, (b&e) immersion time and (c&f) number of coatings of GO solution and CNTs solution

3.3 Characteristics of Coated 3DSWFs

The morphology of uncoated 3DSWF, rGO/3DSWFs, CNTs/3DSWFs, rGO@CNTs/3DSWFs and rGO/CNTs/3DSWFs has been characterized by SEM (Fig. 4). Before coating, 3DSWF is found white and the surface of yarns is smooth without conductive particles, with only sporadic impurities adhered to it [Figs 4 (a) & (b)]. While the surface of yarn becomes rougher after coating [Figs 4 (c)-(f)].

Figure 4 (c) shows that rGO covers the yarn and connects adjacent yarns, it's specific surface area is large and relatively plat, and presents the two-dimensional tulle structure. Meanwhile, it can be observed that there are large multi-layer rGO aggregation structure in some areas. Figure 4 (d) presents the SEM images of CNTs/3DSWFs. After coating, the CNTs wraps the yarns and its aggregates are filled in the yarn gaps.

For rGO@CNTs/3DSWFs, because of the in-one-bath preparation, the overall concentration of the immersion solution is high. Hence, the viscosity also increases, leading to a question of whether the conductive materials are uniformly mixed in the immersion solution, or there are agglomerated conductive materials in the immersion solution, which seriously affects the coating and samples performance. As shown in Fig. 4 (e), there is large area of layered structure on and between yarns, which hides the furrows caused by interweaving between weft and warp yarns. This large layered structure is composed of multiple layer, and there are irregular ripples and curls on the surface.

For rGO/CNTs/3DSWFs, due to the layer-by-layer assemble preparation, rGO and CNTs can be applied seperately and alternately on the 3DSWFs, in the structure of the coating. One-dimensional CNTs serves as an interlayer spacer, effectively separate the two-dimensional rGO sheet to limit their high-dense restacking, which produces a micro-3DSWF like framework with 'surface layer' and 'spacer'. As presented in Fig. 4 (f), the yarns are coated by a mixture of lamellar rGO and linear CNTs, similar to the rGO@CNTs/3DSWFs, but its covering area is not so big and the surface is rougher. Besides irregular folds and crimping, there are also randomly arranged bumps on the surface, which is formed by random aggregation of alternating coated rGO and CNTs.

3.4 Conductive Performance of Coated 3DSWFs

As an insulator, the conductivity of 3DSWFs is tested after impregnating it with conductive coating. Then according to test results, whether the conductive

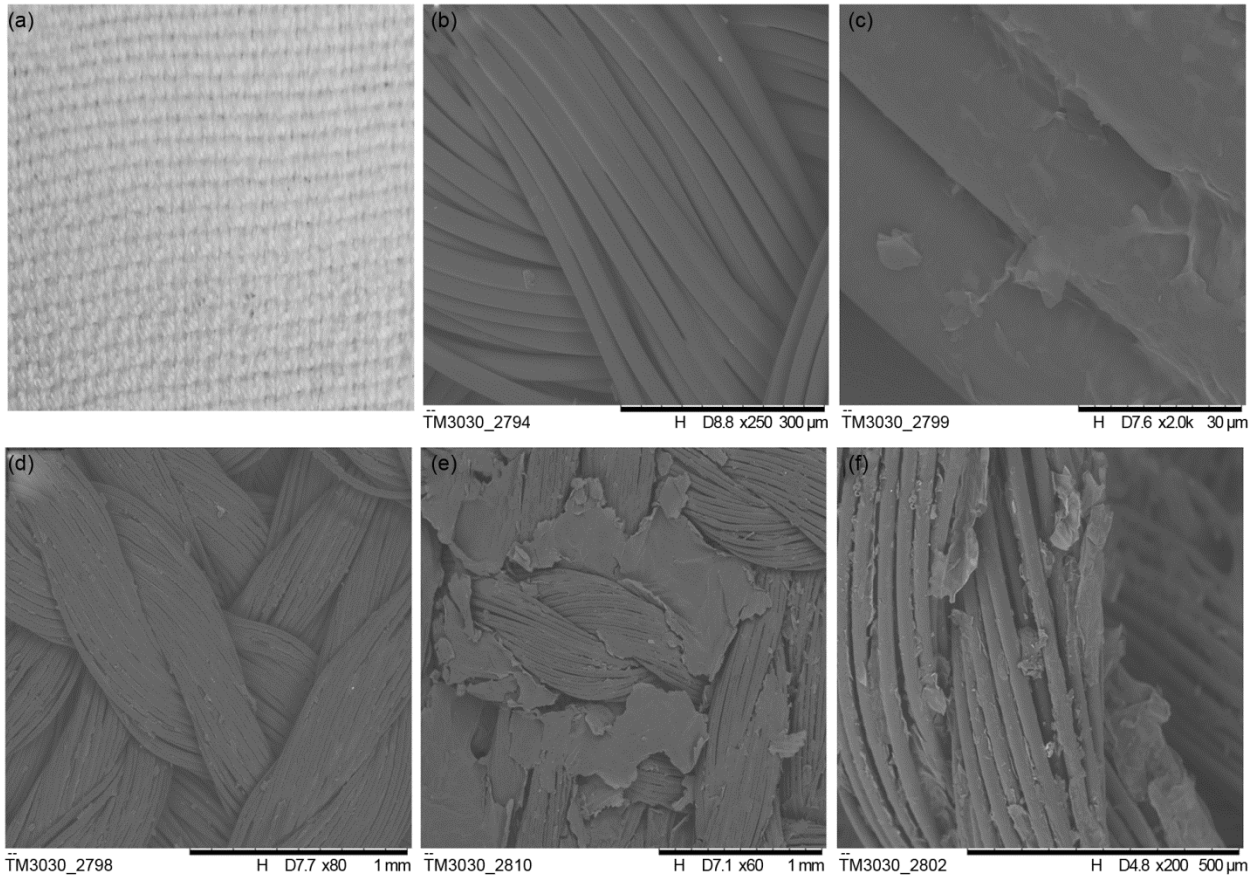

Fig. 4 — Physical photographs (a); and SEM images of 3DSWF before and after coating (b) uncoated 3DSWF, (c) rGO/3DSWFs, (d) CNTs/3DSWFs, (e) rGO@CNTs/3DSWFs, and (f) rGO/CNTs/3DSWFs

materials has formed a complete conductive network on the 3DSWFs, can be determined. Taking resistivity as an example, the higher the resistivity, the more incomplete is the network. So, the ability of 3DSWFs to transport charge is worse, and vice versa. The PTS-9 type four-probe meter has been used to measure the electrical conductivity and resistivity of coated 3DSWFs, the average resistivity obtained are shown in Fig. 5.

In the comparision between samples, the resistivity of the coated 3DSWFs with nine depositions of rGO@CNTs is found the lowest (112.9 Ω·cm), followed by the coated 3DSWFs with six depositions of rGO/MWCNTs (404.2 Ω·cm), CNTs/3DSWFs (2601.3 Ω·cm) and finally rGO/3DSWFs (1961.8 Ω·cm). The resistivity of coated 3DSWFs exhibites a decline by an order of magnitude, when the two conductive materials (rGO and CNTs) act together to achieve the effect of '1+1>2' , which means that using the two conductive materials together is conducive to the improvement in the conductivity of coated 3DSWFs[35,36]. Because the two conductive

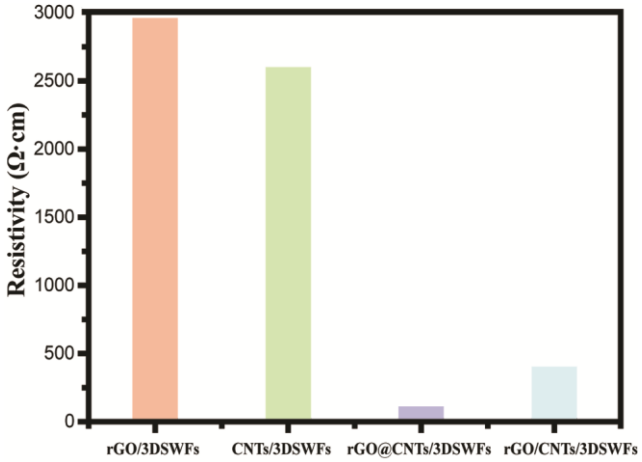

Fig. 5 — Electrical conductivity test results of coated 3DSWFs

materials with different structures will have a synergistic effect when used together, to achieve their complementary effect; one-dimensional CNTs preventes the two-dimensional rGO layers from restacking and forms a bridge between rGO adjacent layers to transport free electrons. They overlaps and

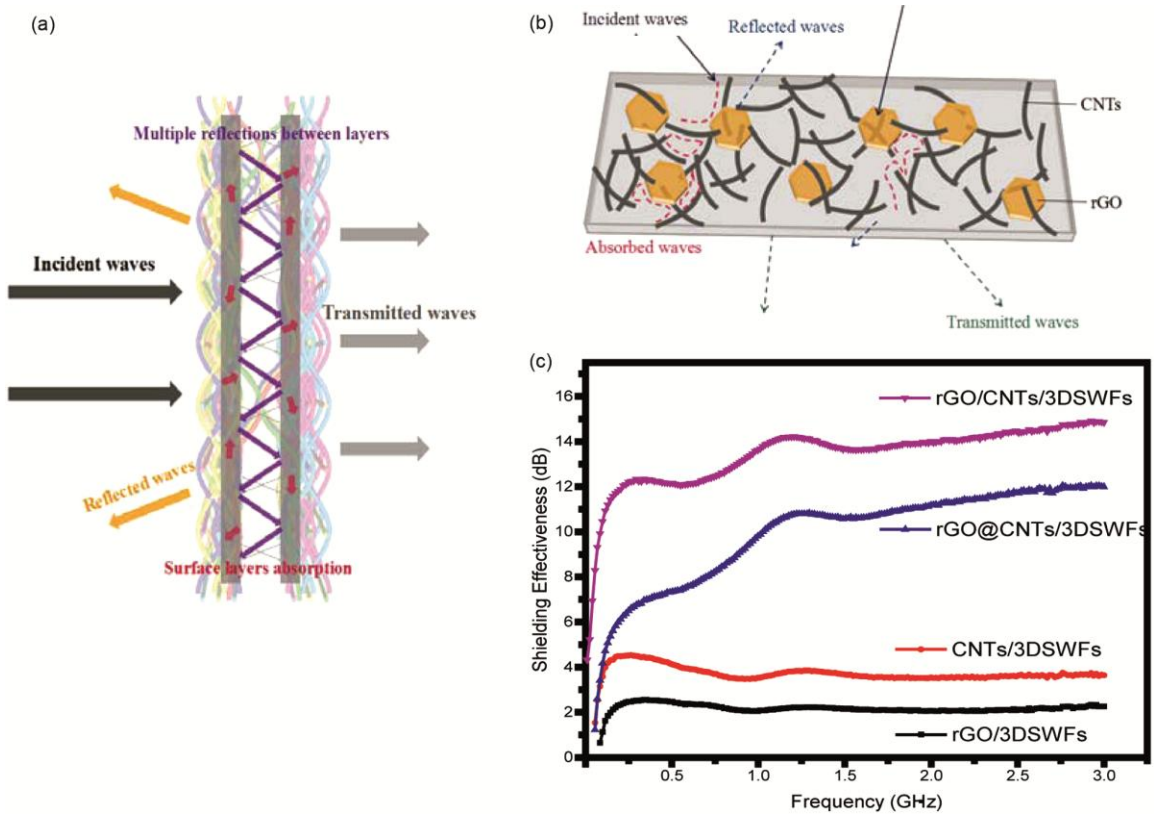

Fig. 6 — EMI shielding mechanism of coated 3DSWFs (a) & (b); and (c) EMI SE of coated 3DSWFs prepared in two methods

interwine with each other to form a more effective three-dimensional network structures and complete conductive path on 3DSWFs, preventing from restacking and providing electronic transport in both horizontal and vertical directions to reduce the resistivity. This is similar to the conclusion obtained in the previous literature[37,38].

Additionally, it was confirmed that conductive network has been formed by impregnating 3DSWFs with rGO, CNTs, rGO@CNTs and rGO/CNTs. The samples are respectively used as wires to access the simple circuit, and the results show that no matter which sample is used, the small light bulb in this series circuit is illuminated when the switch was turned on, which proved that these four conductive materials can form the electrical conductive layer on the 3DSWFs by simple dipping-drying method. The above results indicate that the 3DSWFs designed by our research group has the potential to be applied in flexible wearable electronic devices after coated by conductive materials.

3.5 EMI Shielding Performances of Coated 3DSWFs

The EMI shielding mechanism of the coated 3DSWFs is shown in Figs 6 (a) & (b). Part of the incident waves will be reflected back when they touch the surface of sample, and the other part will enter into the sample. Due to the hierarchical structure of coating and sample, a large number of interfaces will be generated inside the sample, which will trap the waves and form multiple reflections to increase the absorption loss. The remaining part of waves will be transmitted out. The shielding effect of a material against the electromagnetic wave can be expressed by shielding effectiveness (SE), whose unit is decibel (dB). The greater the value, the better is the shielding effect. It can be calculated by following formula:

$$SE = 10 \times \log \frac{p_0}{p_1}$$

where p_0 and p_1 are the power of incident waves and transmitted waves respectively. The EMI shielding performance of coated 3DSWFs with two conductive material are evaluated in the frequency range 0-3 GHz, as displayed in Fig. 6 (c).

For the conductive type EMI shielding materials, electrical conductivity is one of the key factors affecting the shielding performance, i.e. the conductivity of materials is positively correlated with

it's EMI SE. Therefore, according to the test results of the sample's electrical cononductivity, we prespect the EMI SE ranking of the sample to be consistent with it, as shown below:
rGO@CNTs/3DSWFs > rGO/CNTs/3DSWFs > CNTs/3DSWFs > rGO/3DSWFs.

As shown in Fig. 6 (c), if we compare coated 3DSWFs with one conductive material only, the EMI SE values of rGO/3DSWFs and CNTs/3DSWFs are 2 dB and 4 dB respectively. CNTs/3DSWFs have higher SE, which is exactly what we predicted. At the same time, it is found that no matter which preparation method is adopted, the SE values of coated 3DSWFs with rGO and CNTs are found higher than the sum of SE of rGO/3DSWFs and CNTs/3DSWFs, which indicates that there is a synergistic effect between rGO and CNTs. By comparing the four kinds of samples, it is found that the SE of two-component conductive materials coating 3DSWFs (15 dB and 12 dB respectively) is much higher than that of single-component conductive materials coating 3DSWFs (2 dB and 4 dB respectively), because the combination of two conductive materials with different structures is conducive to the formation of a complete conductive path and a large number of interface. When the incident electromagnetic waves contact the sample, the complete conductive network will generate current and lead to ohm loss. Besides, a large number of interfaces will cause multiple reflections to attenuate the incident electromagetic waves and increase the absorption loss.

The SE of coated 3DSWFs with two conductive materials prepared by different methods has been compared. The SE of rGO/CNTs/3DSWFs and rGO@CNTs/3DSWFs are 15 dB and 12 dB respectively. In layer-by-layer assembly method, the two materials can form more hierarchical interfaces on 3DSWFs, which is not only conducive for the purpose of uniform diposition, but also for achieving their complementary effect. When incident electromagnetic waves touch 3DSWFs, it will be more interfered in its propagation path. When the in-one-bath method is used, the impregnation solution is more viscous than others, as both rGO and CNTs are easy to accumulate and agglomerate. The rGO and CNTs in the solution may not be completely uniformly dispersed, leading to the phenomenon of uneven coating. It is found that the result is different from that of the predicted result. This indicates that the electrical conductivity of sample is positively correlated but not fully proportional to its EMI shielding performance. The EMI shielding performance is also related to the type of conductive material, preparation method and other factors.

4 Conclusion

In this research, we designed a novel 3DSWF fabric. The upper and lower layers of 3DSWF are of interlaminar orthogonal structure, and the spacing yarns connect the two layers with the shape of 'X'. In order to make it adapt to more diverse needs, it's given electrical conductivity to broaden its application.

4.1 The single factor analysis method has been used to determine the preparation parameters of conductive treated 3DSWFs. The preparation parameters are set as follow: GO concentration 3 mg/mL, immersion time 2 h and number of coating layers 9. When the layer-by-layer assembly method is used, CNTs concentration is 2 mg/mL, the immersion time is 30 min and the number of coating layers is 6.

4.2 The resistivity test results of the coated 3DSWFs show that the synergistic effect between rGO and CNTs gives the excellent electrical performance. Compared to the 3DSWFs coated with rGO or CNTs, the resistivity of the 3DSWFs coated with both rGO and CNTs can be reduced by an order of magnitude.

4.3 The influence of two different preparation methods on electrical conductivity and EMI SE of the samples has also been analyzed. The result shows that the EMI SE of rGO/CNTs/3DSWFs obtained by layer-by-layer assembly coating with 6 layers (15 dB) is higher than that of rGO@CNTs/3DSWFs obtained by in-one-bath coating with 9 layers (12 dB). This indicates that the synergistic effect between rGO and CNTs can be better reflected by layer-by-layer assemble method.

4.4 The resistivity of rGO@CNTs/3DSWFs is lower than that of rGO/CNTs/3DSWFs, which is 112.9 Ω·cm and 404.2 Ω·cm respectively. But the latter has better EMI shielding property, which is different from the expected. The results suggest that the electrical conductivity of sample is positively correlated but not fully proportional to its EMI shielding performance, and the preparation method is also one of the influencing factors.

4.5 This study provides idea for the design and preparation of 3DSWF, expand the application field

of the 3DSWF and provides reference value for the further development of multi-functional materials based on the 3DSWF.

References

1 Hongji Duan, Mingjuan Zhao, Yaqi Yang, Guizhe Zhao & Yaqing Liu, *Materials Sci: Materials in Electronics*, 12(2018)29.

2 Lihua Zou, Chuntao Lan, Li Yang, Zhenzhen Xu, Changliu Chu, Yingcun Liu & Yiping Qiu, *Diamond Related Materials*, 104(2020)107757.

3 Sage Cindy & Burgio Ernesto, *Child Development*, 1(2018)89.

4 Qi Q, Wang Y, Din X, Wang W, Xu R & Yu D, *Appl Organometal Chem*, 34(2020)e5434.

5 Teber A , Unver I, Kavas H & Akts B & Bansal R, *J Magnetism Magnetic Materials*, 406(2016) 228.

6 Yan Zhang, Wenxiang Tian, Longxiang Liu, Wenhua Cheng, Wei Wang, Kim Meow Liew, Bibo Wang & Yuan Hu, *Chem Eng J*, 372(2019)1077.

7 Young-Woo Nam, Jae-Hun Choi, Won-Jun Lee & Chun-Gon Kim, *Composite Structures*, 160(2017)1171.

8 Siyi Bi, Hang Zhao, Lei Hou & Yinxiang Lu, *Appl Surface Sci*, 419(2017)465.

9 Lan Chuntao, Guo Min, Li Chenglong, Qiu Yiping, Ma Ying & Sun Junqi, *ACS Appl Materials Interfaces*, 6(2020)12.

10 Guang Yin, Yu Wang, Wei Wang & Dan Yu, *Colloids Surfaces A: Physicochem Eng Aspects*, 601(2020)125047.

11 Wang C, Guo R, Lan J, Tan L, Jiang S & Xiang C, *J Materials Sci: Materials Electronics*, 29(10) (2018)1.

12 Zhao H, Hou L Bi S & Luy, *ACS Appl Mater Interfaces*, 38(9) (2017)33059.

13 Zhonglei Ma, Songlei Kang, Jianzhong Ma, Yali Zhang, Liang Shao, Ajing Wei, Xiaolian Xiang, Linfeng Wei & Junwei Gu, *ACS Nano*, 14(2020) 8368.

14 Ilhwan Yu, Jaehyoung Ko, Tea-Wook Kim, Dong Su Lee, Nam Dong Kim, Sukang Bae, Seoung-Ki Lee, Jaewon Choi, Sang Seok Lee & Yongho Joo, *Carbon*, 167(2020)523.

15 Du D, Tang Z & Ouyang J, *J Materials Chem C*, 6(2018)883.

16 Chen L, Guo K, Zeng S L & Xu L, Xiang C-Y, Zhang S & Li B-J, *Carbon*, 162(2020)445.

17 Xu C, Zhao J, Chao Z, Wang J, Wang W, Zhang X & Li Q, *Composites Communi*, 21(2020)100409.

18 Shahzad Faisal, Kumar Pradip, Kim Yoon-Hyun, Hong Soon Man & Koo Chong Min, ACS *Appl Materials Interfaces*, 14(2016)8.

19 Gupta S, Chang C, Anbalagan A K, Lee C-H & Tai N, *Composites Sci Technol*, 188(2020)107994.

20 Zhai J, Cui C, Ren E, Zhou M, Guo R, Xiao H, Li A, Jiang S & Qin W, *J Materials Sci Materials Electronics*, 31(2020)8910.

21 Ghosh S, Ganguly S, Das P, Das T K, Bose M, Singha N K, Das A K & Das N C, *Fibers Polym*, (20)6(2019)1161.

22 Liu-Xin Liu, Wei Chen, Hao-Bin Zhang, Qi-Wei Wang, Fanglan Guan & Zhong-Zhen Yu, *Adv Functional Materials*, 44(2019)29.

23 Maya M G, Abraham J, Arif P M, Moni G, George J J, George S C & Thomas S, *Polym Testing*, 87(2020)106525.

24 Chen W, Duan W, Liu Y, Wang Q & Qi F, *Industrial Eng Chem Res*, 58 (47) (2019)21531.

25 Tatjana V Mihailovic, Koviljka A Asanovic & Dragana D Cerovic, *J Sandwich Structures Materials*, 6(2018)20.

26 Seongcheol Ahn, Yujang Cho, Sangki Park, Junseo Kim, Jingzhe Sun, Dahye Ahn, Miyeon Lee, Daeeun Kim, Taeyun Kim, Hangsik Shin & Jong-Jin Park, *Nano Energy*, 74(2020)104932.

27 Ghanshyam Neje & Bijoya Kumar Behera, *Composites Part B*, 160(2019)306.

28 Dominik Krumm, Stefan Schwanitz & Stephan Odenwald, *Appl Ergonomics*, 86(2020)103099.

29 Razieh Abedkarimi, Hossein Hasani, Parham Soltani & Zahra Talebi, *Text Inst*, 4(2020)111.

30 Ying Sheng, Le Zhang, Yanqiang Wang & Zhuangzhuang Miao, *Building Environment*, 177(2020)106903.

31 Muhammad Umair, Syed Talha Ali Hamdani, Yasir Nawab, Muhammad Ayub Asghar, Tanveer Hussain & Abdelghani Saouab, *Fibers Polym*, 6(2019)20.

32 Liyong Wang, Kun Zhang, Farial Islam Farha, Huan Ma, Yiping Qiu & Fujun Xu, *J Materials Sci*, 6(2020)55.

33 Pan Y J, Lou C W, Hsieh C T, Huang C H, Lin Z I, Li C W & Lin J H, *Fibers Polym*, 17 (2016)789.

34 Wang H, Li T T, Wu L, Low C W & Lin J H, *Materials*, 11(2018)11.

35 Nuray Ucar, Burçak Karagüzel Kayaoğlu, Arınc Bilge, Gunseli Gurel, Pınar Sencandan & Selcuk Paker, *J Composite Materials*, 24(2018)52.

36 Rumiana Kotsilkova, Evgeni Ivanov, Vladimir Georgiev, Radost Ivanova, Dzhihan Menseidov, Todor Batakliev, Verislav Angelov, Hesheng Xia, Yinghong Chen, Dzmitry Bychanok, Polina Kuzhir, Rosa Di Maio, Clara Silvestre & Sossio Cimmino, *Polymers*, 6(2020)12.

37 Yu Yang, Qiyao Huang, Liyong Niu, Dongrui Wang, Casey Yan, Yiyi She & Zijian Zheng, *Adv Materials*, 19(2017)29.

38 Zhou Zehang, Panatdasirisuk Weerapha, Mathis Tyler S, Anasori Babak, Lu Canhui, Zhang Xinxing, Liao Zhiwei, Gogotsi Yury & Yang Shu, *Nanoscale*, 13(2018)10.